Quasar Outflows and AGN Feedeback: The TMT Revolution

Nahum Arav

Virginia Tech

Collaborators:

Benoit Burguet
Carter Chamberlin
Doug Edmonds
Jerry Kriss
Jelle Kaastra
Max Moe
Jay Dunn
Kirk Korista
Chris Benn
Manuel Bautista
Eric Hallman
Elisa Costantini
Kentaro Aoki

Artistic Credit:
ESO/L. Calçada

Talk outline

- **Punchline:**

Luminous quasars have sub-relativistic (~10^4 km/s) absorption outflows with:

- Large scale (~1000 pc.), large mass flow rate (~300 $M_\odot$/yr)

- Kinetic luminosity sufficient for AGN feedback processes

- **The empirical evidence and its caveats**

- **The revolutionary potential of the TMT for this research**

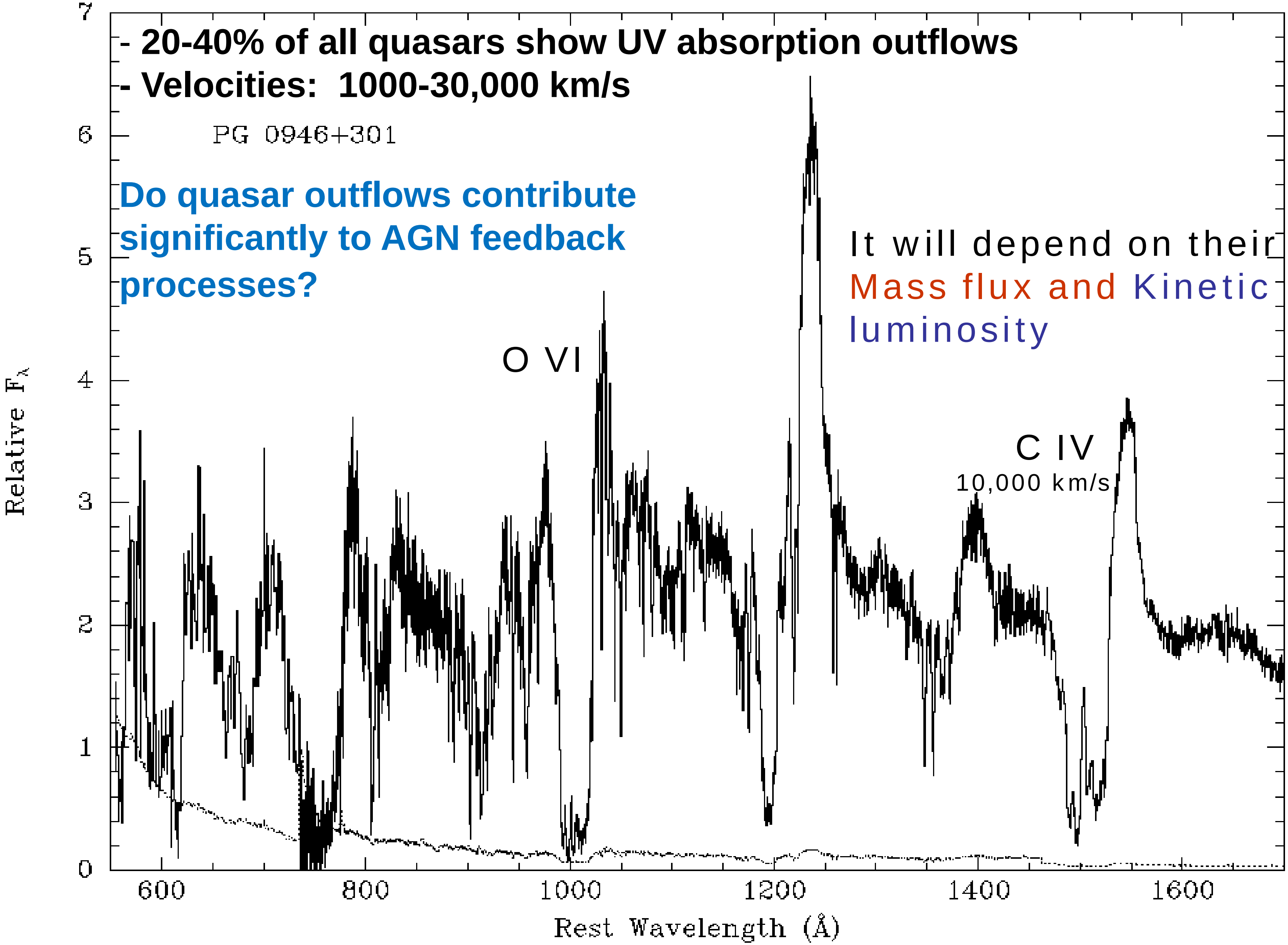
- 20-40% of all quasars show UV absorption outflows
- Velocities: 1000-30,000 km/s
PG 0946+301
Do quasar outflows contribute significantly to AGN feedback processes?
It will depend on their Mass flux and Kinetic luminosity
O VI
C IV
10,000 km/s
Relative F_λ
Rest Wavelength (Å)
0
1
2
3
4
5
6
7
600
800
1000
1200
1400
1600

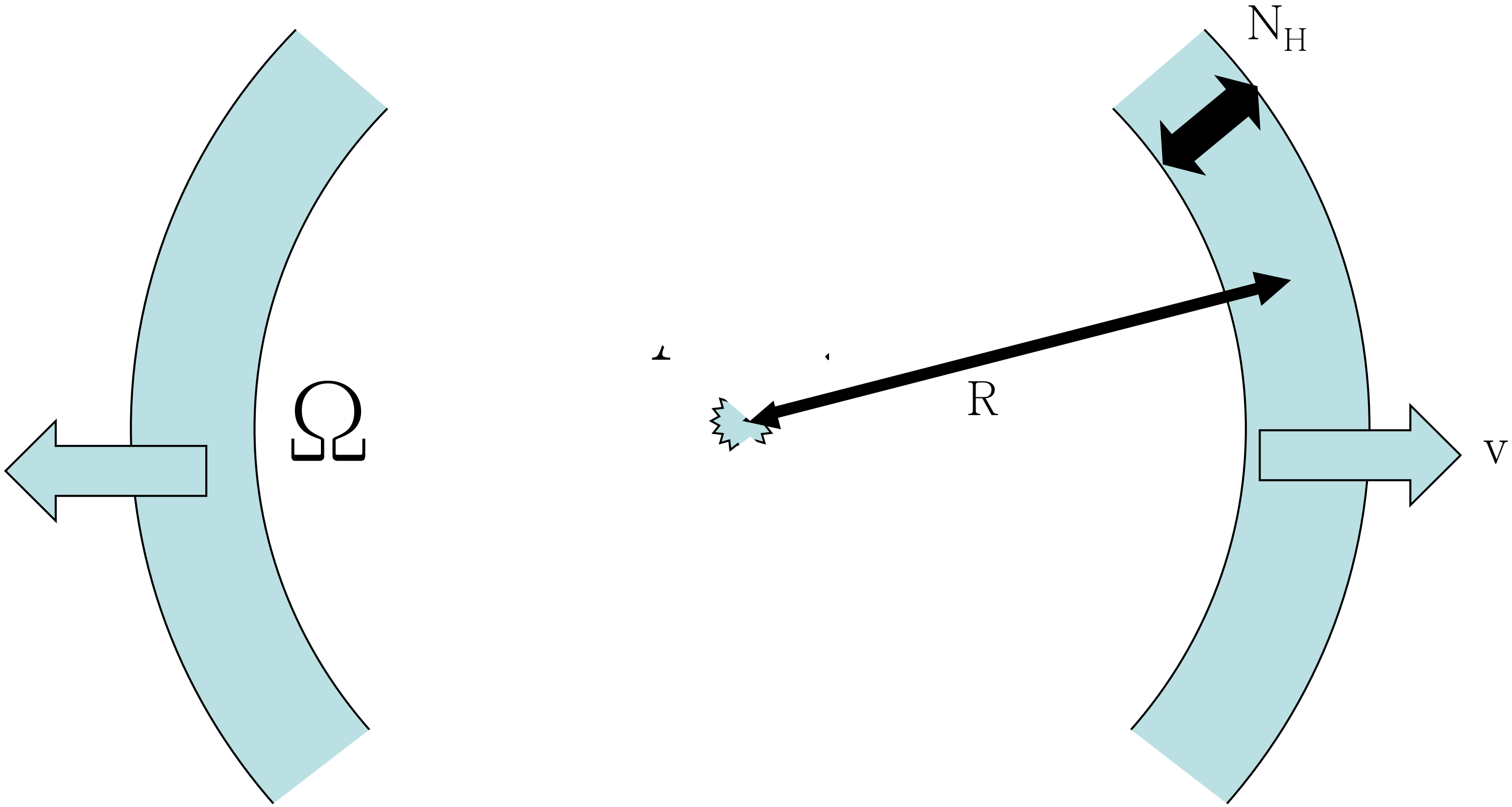

N_H
Ω
R
v

Mass flux and Kinetic luminosity of absorption outflows

$$M \simeq 4\pi\Omega R^2 N_H \mu m_p \qquad \dot{M} \equiv \frac{M}{(R/v)} = 4\pi\Omega R N_H \mu m_p v \qquad \dot{E}_k = \frac{1}{2}\dot{M} v^2$$

$$\dot{E}_k = \frac{1}{2}\dot{m}v^2 \approx 2\pi\Omega R N_H 1.4 m_p v^3$$

Up until 2008:

$$N_H \approx 10^{20-24}\, cm^{-2}$$

$$R \approx 0.01 - 10000\, pc$$

$$\Omega \approx 0.2$$

Exceptions: De Kool + (3 objects); Hamann 3c191

Hewett & Foltz. 2003
Trump + 2006
Dai + 2008

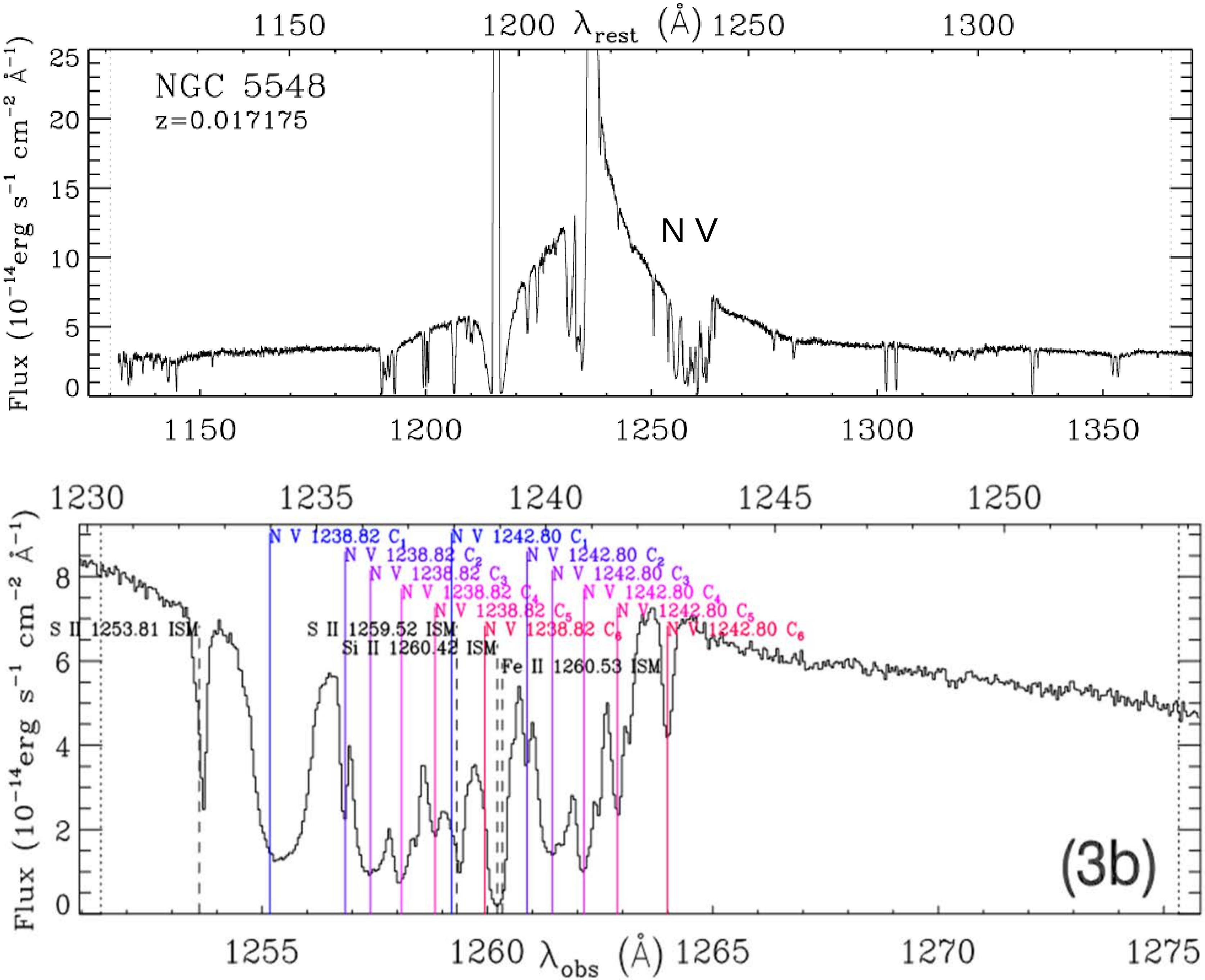

NGC 5548
z=0.017175
N V
λrest (Å)
Flux (10⁻¹⁴erg s⁻¹ cm⁻² Å⁻¹)
N V 1238.82 C1
N V 1238.82 C2
N V 1238.82 C3
N V 1238.82 C4
N V 1238.82 C5
N V 1238.82 C6
N V 1242.80 C1
N V 1242.80 C2
N V 1242.80 C3
N V 1242.80 C4
N V 1242.80 C5
N V 1242.80 C6
S II 1253.81 ISM
S II 1259.52 ISM
Si II 1260.42 ISM
Fe II 1260.53 ISM
λobs (Å)
(3b)

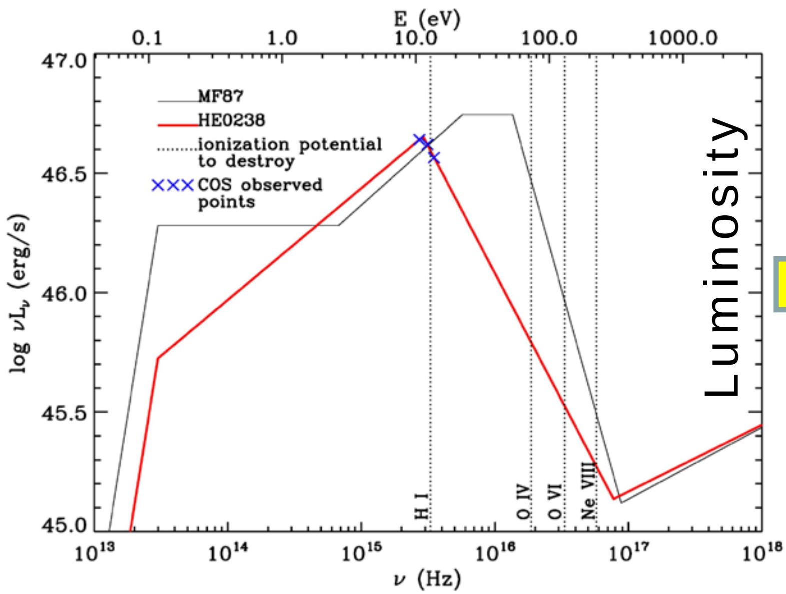

Frequency

Cloudy

Column densities

Table S1: UV column densities for the outflow components in NGC 5548

Ion	v_1 [−1450, −850][a]	v_2 [−850, −750]	v_3 [−750, −540]	v_4 [−540, −360]	v_5 [−360, −80]	v_6 [−80, +50]
			Epoch 2013			
H I	>14.39[b]	>13.86	>14.28	>14.40	>14.00	>13.00
C II	>14.13	<12.81	<13.21	<13.24	<13.40	<13.00
C IV	>14.60	$14.00^{+0.3}_{-0.1}$	>14.30	>14.30	>14.10	>13.70
N V	>14.90	$13.90^{+0.2}_{-0.2}$	>14.90	>14.80	>14.60	>14.10
Al II	>13.05					
Si II	$14.30^{+0.18}_{-0.3}$	<11.80	<12.00	<11.90	<11.40	<12.10
Si III	>13.70	<12.00	$13.10^{+0.3}_{-0.3}$	<12.20	$12.20^{+0.2}_{-0.2}$	<11.50
Si IV	>14.08	$12.30^{+0.2}_{-0.2}$	$13.88^{+0.2}_{-0.2}$	<13.00	$13.13^{+0.2}_{-0.2}$	<12.30
P III	$14.04^{+0.16}_{-0.06}$					
P V	$14.15^{+0.5}_{-0.15}$					
S III	$15.00^{+0.30}_{-0.22}$					
Fe III	$14.70^{+0.30}_{-0.30}$					
			Epoch 2011			
H I	>14.34	>13.80	>14.28	>14.33	>13.83	>12.90
C IV	>14.20	>13.70	>14.30	$14.40^{+0.2}_{-0.2}$	>13.83	>13.03
N V	>14.59	>13.95	>14.65	>14.77	>14.43	>13.84
Si III	<12.20	<11.50	<11.98	<11.84	<11.55	<11.59
Si IV	<13.06	<12.54	<12.66	<12.70	<12.53	<12.37
			Epoch 2004			
H I	>13.94	>13.82	>14.20	>14.44	>14.15	>12.41
C IV	>14.59	>13.83	>13.95	>14.25	>14.20	>13.16
N V	>14.65	>13.83	>14.20	>14.35	>13.75	>13.20
Si III	>13.20	>12.47	>13.29	>12.41	>12.66	>12.33
Si IV	>14.18	>12.91	>13.65	>12.71	>13.32	>12.76
			Epoch 2002			
H I	>14.34	>13.91	>14.29	>14.46	>13.91	>13.20
C IV	>14.08	>13.54	>13.95	$14.30^{+0.2}_{-0.2}$	>13.60	>13.23
N V	>14.54	$13.87^{+0.2}_{-0.2}$	$14.50^{+0.2}_{-0.2}$	>14.76	>14.12	>13.21
Si III	<12.66	<11.80	<11.97	<11.91	<12.14	<11.97
Si IV	<13.31	<12.39	<12.81	<12.74	<13.13	<12.58
			Epoch 1998			
H I	>14.06	>13.66	>14.28	>14.36	>13.75	>12.96
C IV	<13.69	>13.25	>13.59	>14.47	<13.09	<13.00
N V	<13.99	>13.89	>14.19	>14.88	>14.13	<13.98
Si III	<12.83	<12.14	<12.46	<12.18	<12.57	<12.41
Si IV	<13.39	<12.83	<12.93	<12.69	<12.89	<12.13

[a]Integration limits in km s^{-1}.

[b]Lower limit log column densities given in units of cm^{-2} are shown in blue.

Upper limits are likewise shown in red.

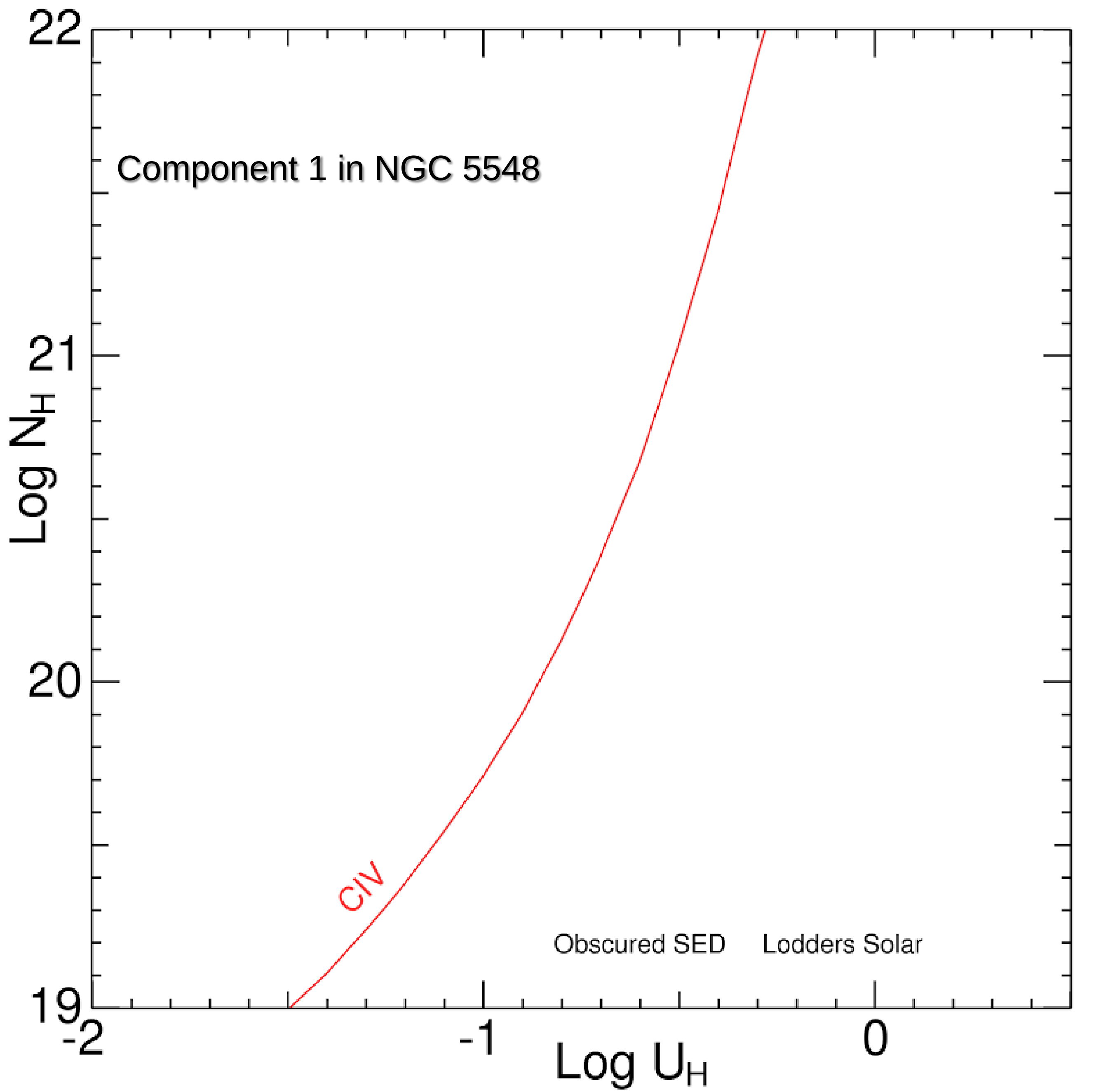
22
21
20
19
-2
-1
0
Log N_H
Log U_H
Component 1 in NGC 5548
CIV
Obscured SED
Lodders Solar

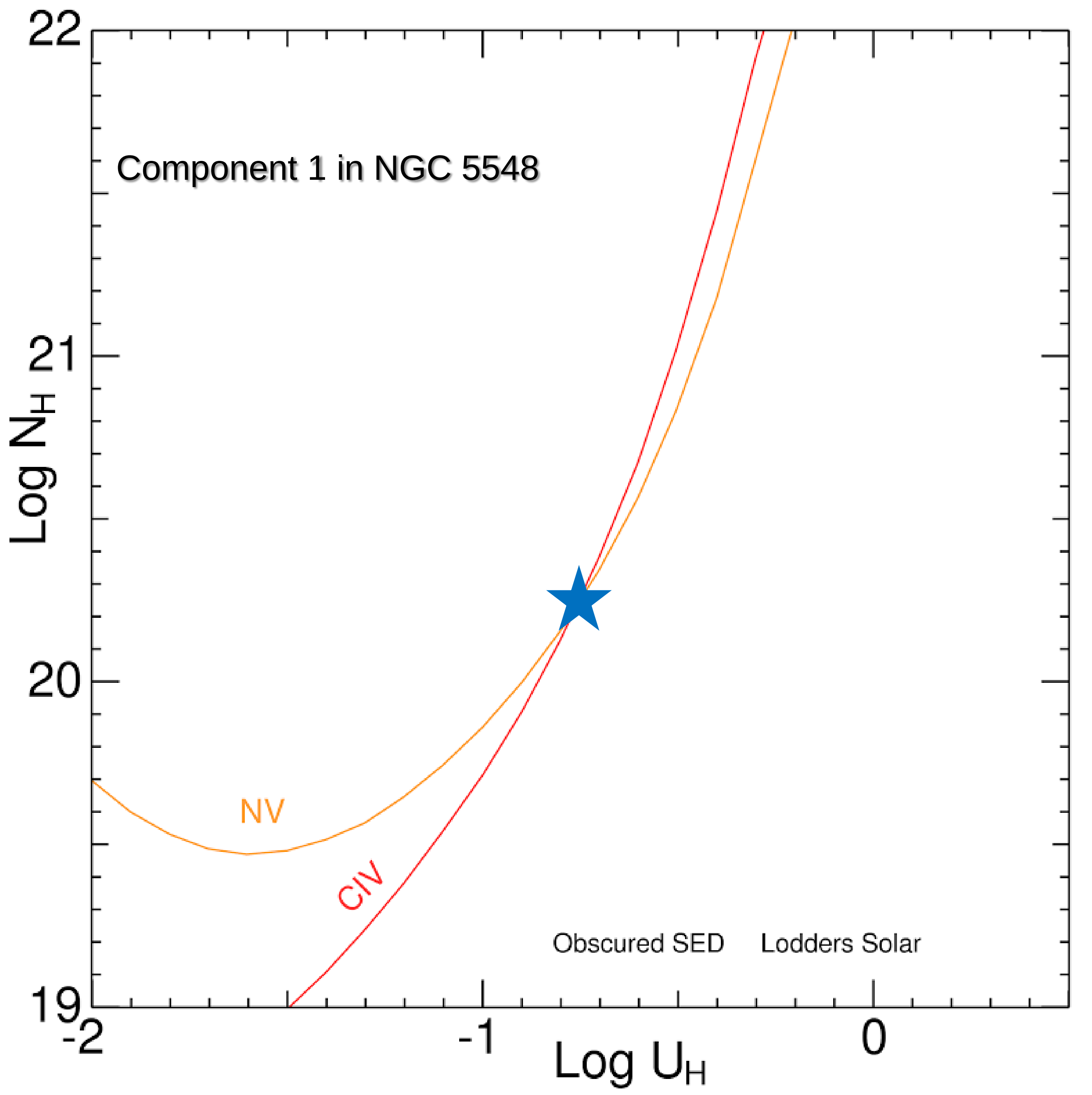

Component 1 in NGC 5548
NV
CIV
Obscured SED
Lodders Solar
Log N_H
Log U_H
22
21
20
19
-2
-1
0

- ✓ 1) Getting reliable N_{ion}
- ✓ 2) Measuring U and N_H
- 3) Determining **R**

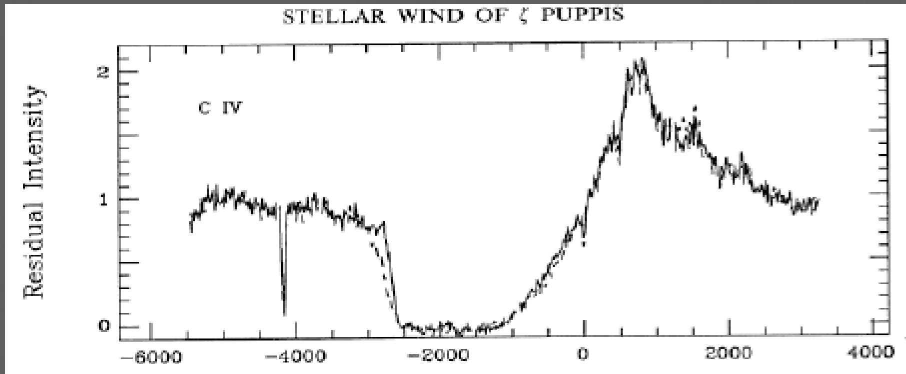

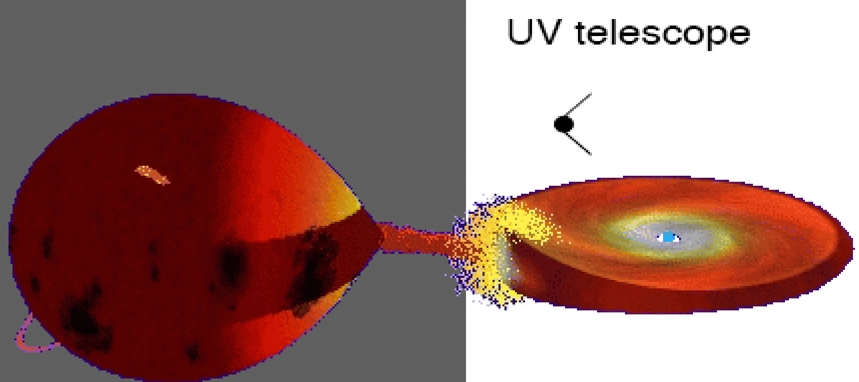

Animation from Stella Kafka's webpage

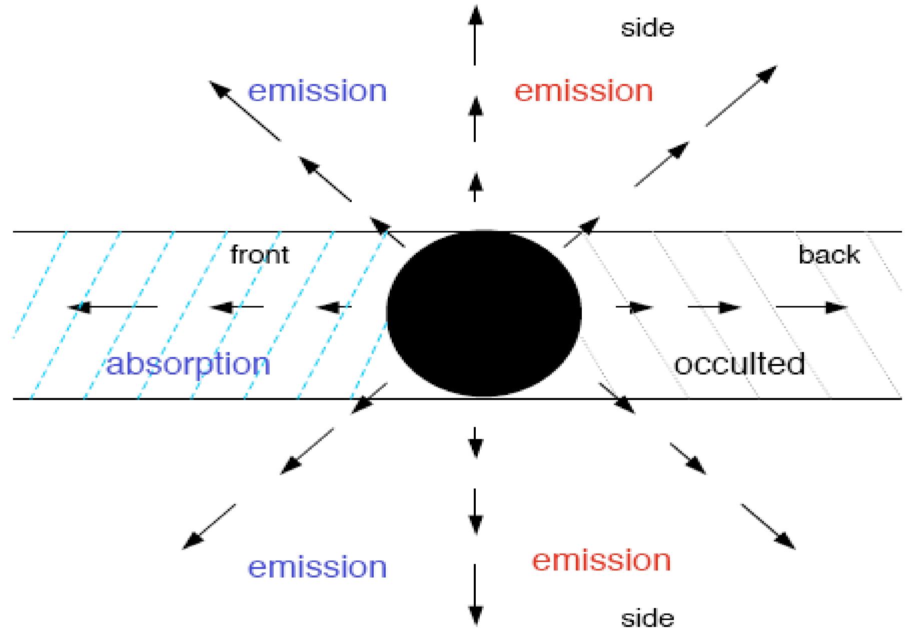

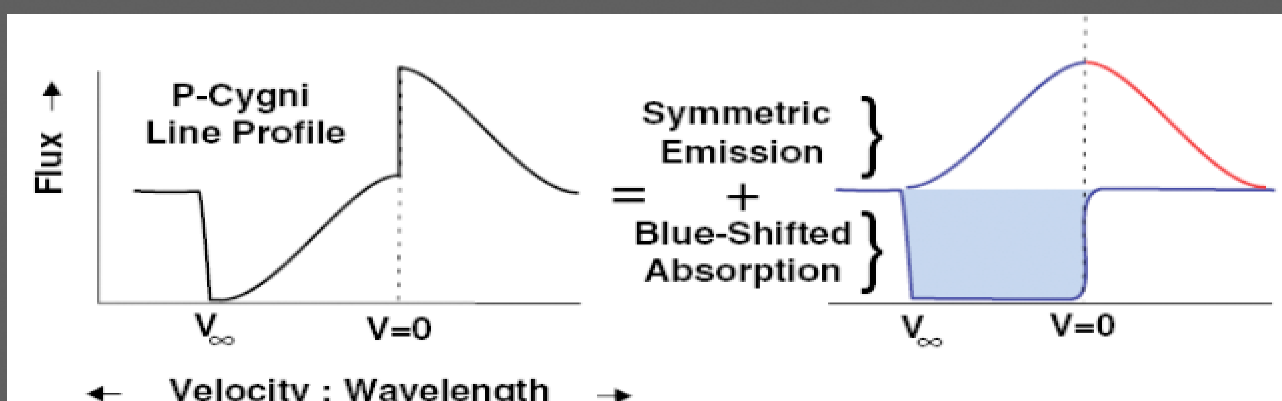

Figure by David Cohen

A Structure for Quasars

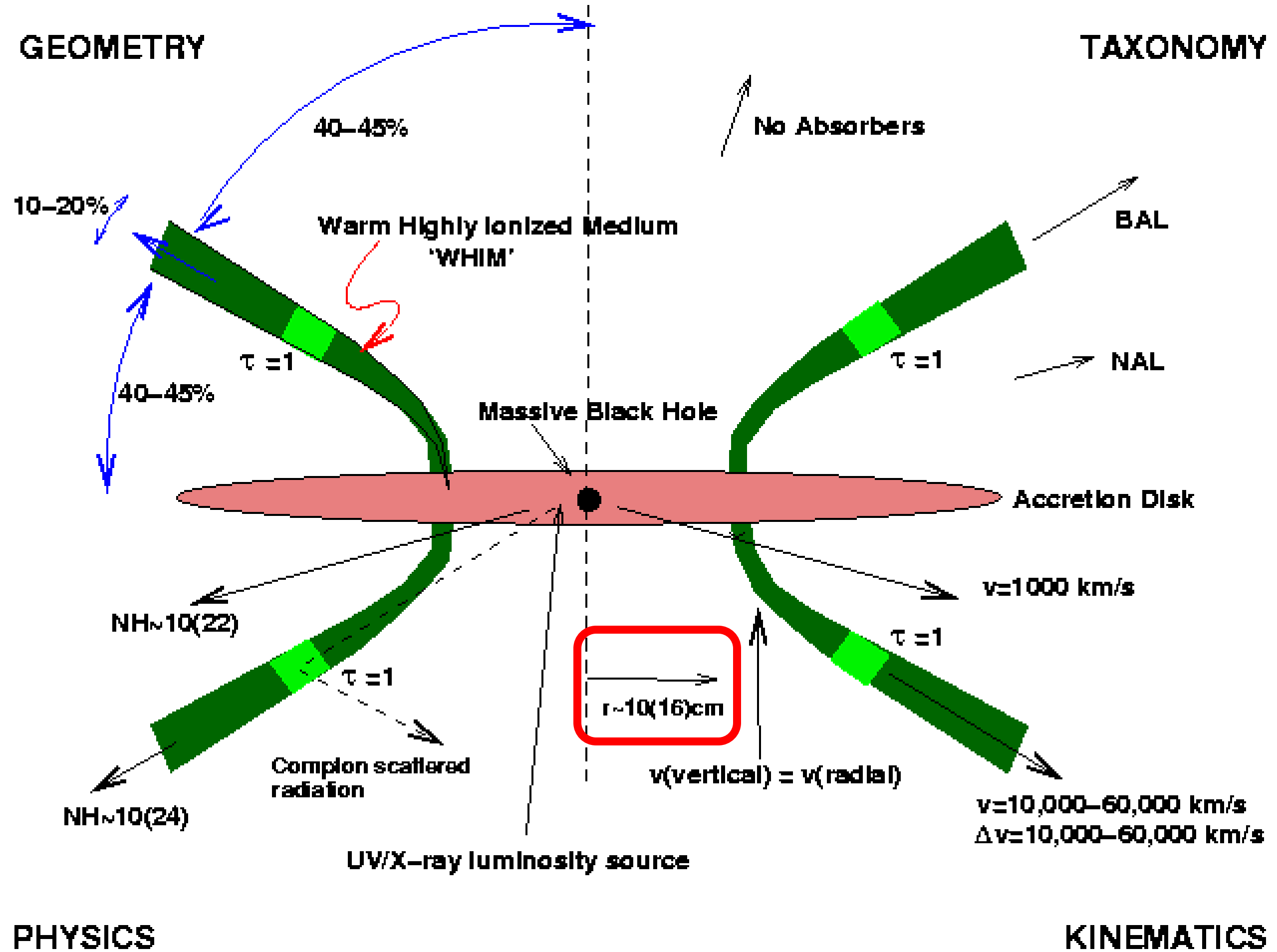

Elvis M. 2000 Ap.J. 545,63. (astro-ph/0008064)

Measuring the distance (R) from the central source to the outflow

$$U_H \equiv \frac{Q_H}{4\pi R^2 c n_e}$$

$$R = \sqrt{\frac{Q_H}{4\pi c n_e U_H}}$$

Best way: Direct imaging
Or better yet IFU observations

Crenshaw + 2000 (series of papers)
Fischer + 2015

Storchi-Bergmann (series of papers)

Liu, Zakamska + 2013a,b,c, 2014

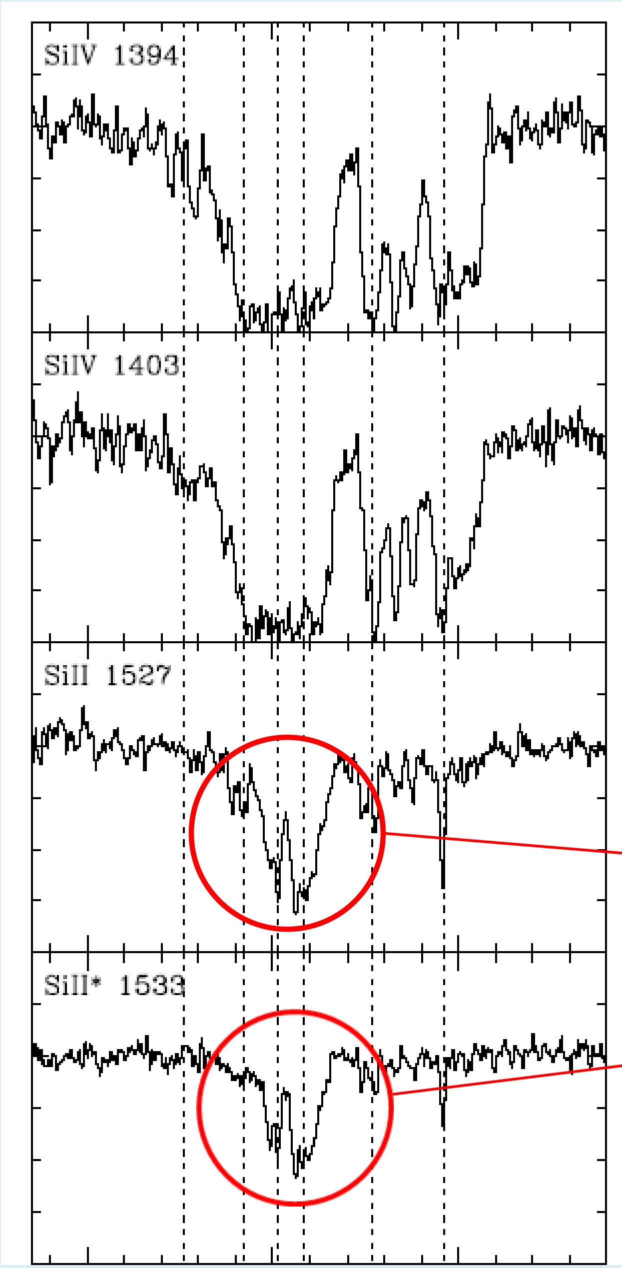

From Hamman + 2001:
High-Resolution Keck Spectra of the Associated Absorption Lines in 3C 191

$$R = \sqrt{\frac{Q_H}{4\pi c n_e U_H}} = 28kpc$$

$$n_e \approx n_{cr} \left(\frac{2\,N_{lo}}{N_{up}} - 1 \right)^{-1} = 300\ \mathrm{cm}^{-3}$$

Si II

The dynamical range of excited states diagnostics

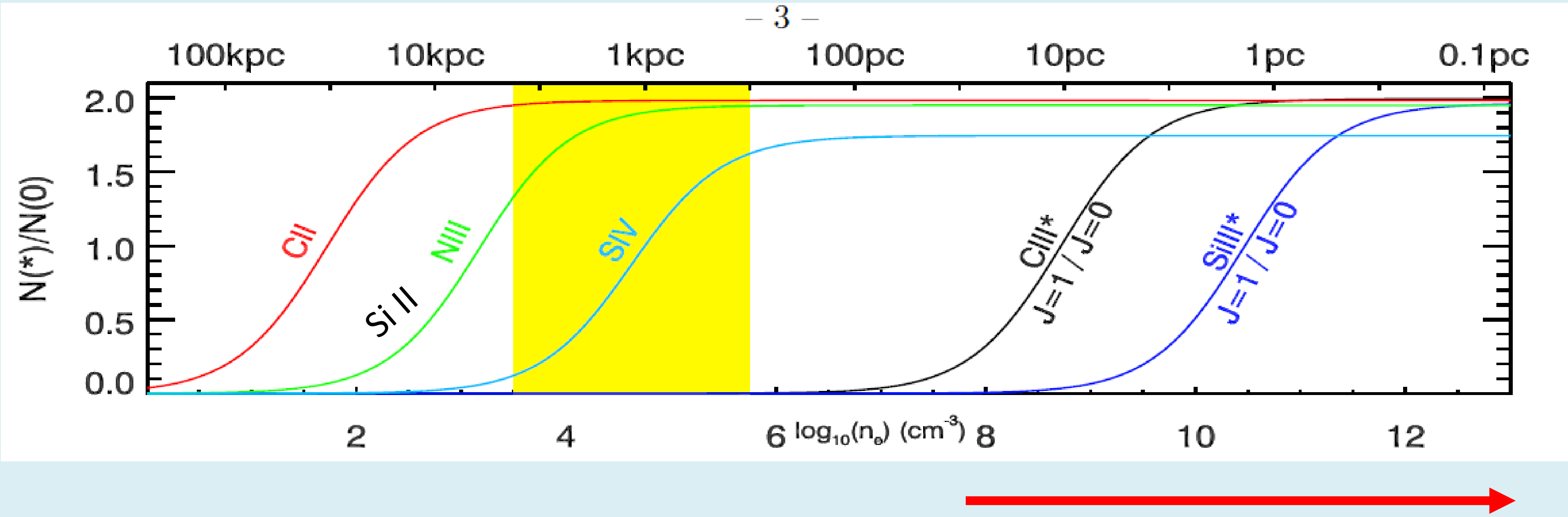

Imaging and IFU observations cannot probe scales<~30 pc

object	Distance (pc)	reference	comments
QSO 3c 191	28,000	Hamann et al (2001)	Si II*/Si II
IRAS-F22456-5125	10,000	Borguet et al (2012a)	Si II*/Si II LLQ
SDSS J0318-0600	6000	Dunn et al (2010)	Si II*/Si II
Akari 1757+5907	3,700	Aoki et al. (2011)	Fe II*/Fe II
SDSS J0838+2955	3,300	Moe et al. (2009)	Fe II*/Fe II
IRAS~F04250-5718	3000	Edmonds et al (2011)	C II*/C II LLQ
QSO HE0238-1904	3000	Arav et al (2013)	**O IV*/O IV**
QSO 2359-1241	1000 (5 comps)	Bautista et al (2010)	Fe II*/Fe II
FBQS J1044+3656	700	de Kool et al. (2001)	Fe II*/Fe II
SDSS J1106+1939	300	Borguet et al (2013)	**S IV*/S IV**
FBQS 0840+3633	230	de Kool et al. (2002a)	Si II*/Si II
Mrk 509	> 200	Arav et al. (2012)	No variability, Seyfert
SDSS J0802 + 5513	200	Ji et al 2015 ApJ, 800, 56	Fe II*/Fe II
SDSS J1512+1119	100 and >2000	Borguet et al (2012b)	**S IV*/S IV**
SDSS J0831+03541	100	Chamberlain et al (2014)	**S IV*/S IV**
FBQS J1151+3822	7-130	Lucy et al (2015)	Fe II*/Fe II
NGC 3783	25	Gabel et al (2005)	C III* Seyfert
FBQS 1214+2803	1-30	de Kool et al. (2002b)	Fe II*/Fe II
NGC 5548	5, 15, 100, >130	Arav et al. (2015)	C III* Seyfert
FBQS 0840+3633	1	de Kool et al. (2002a)	Fe III*

10^3-10^4 pc

10^2-10^3 pc

10^0-10^2 pc

The highest kinetic luminosity Outflow

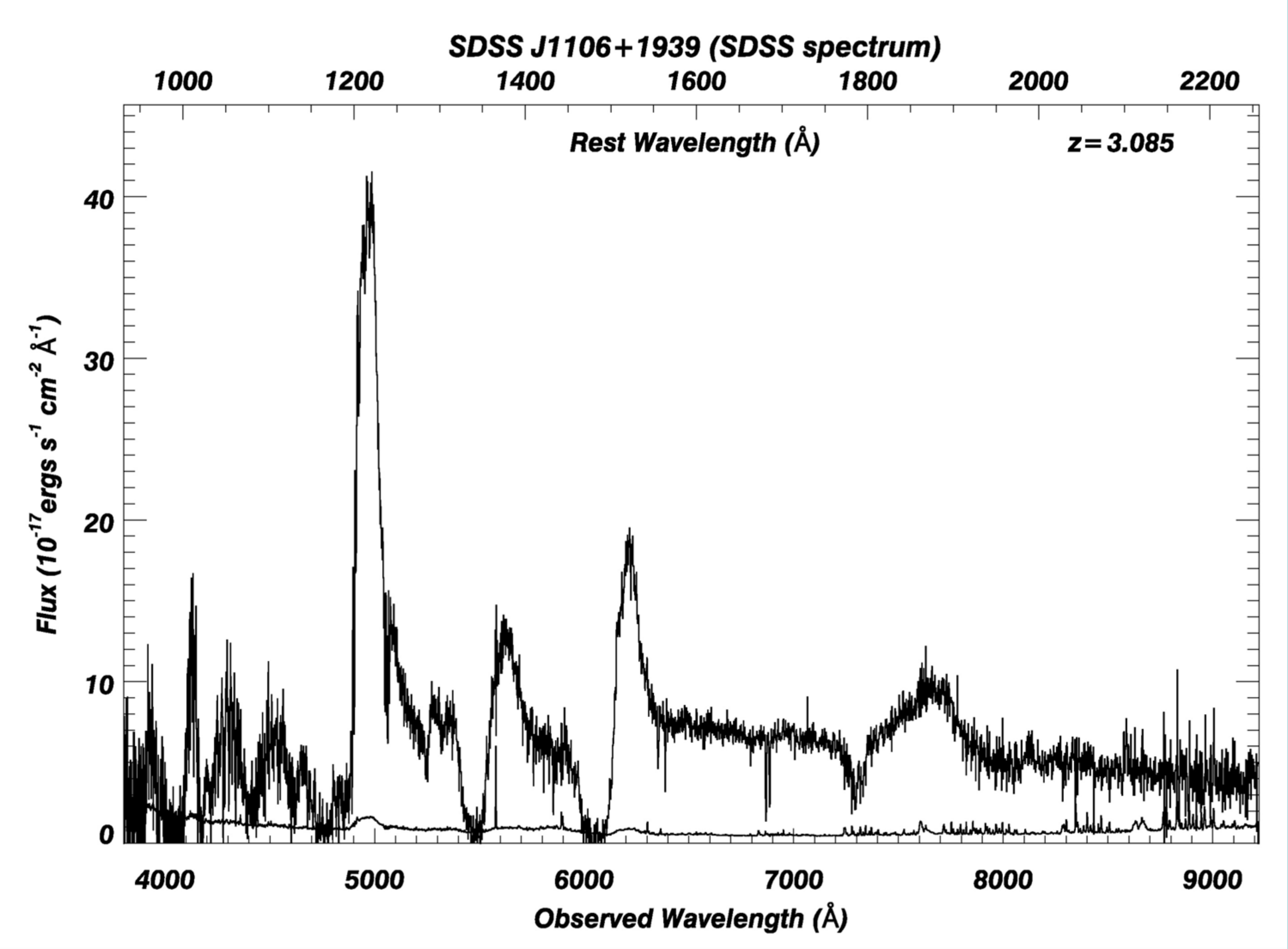

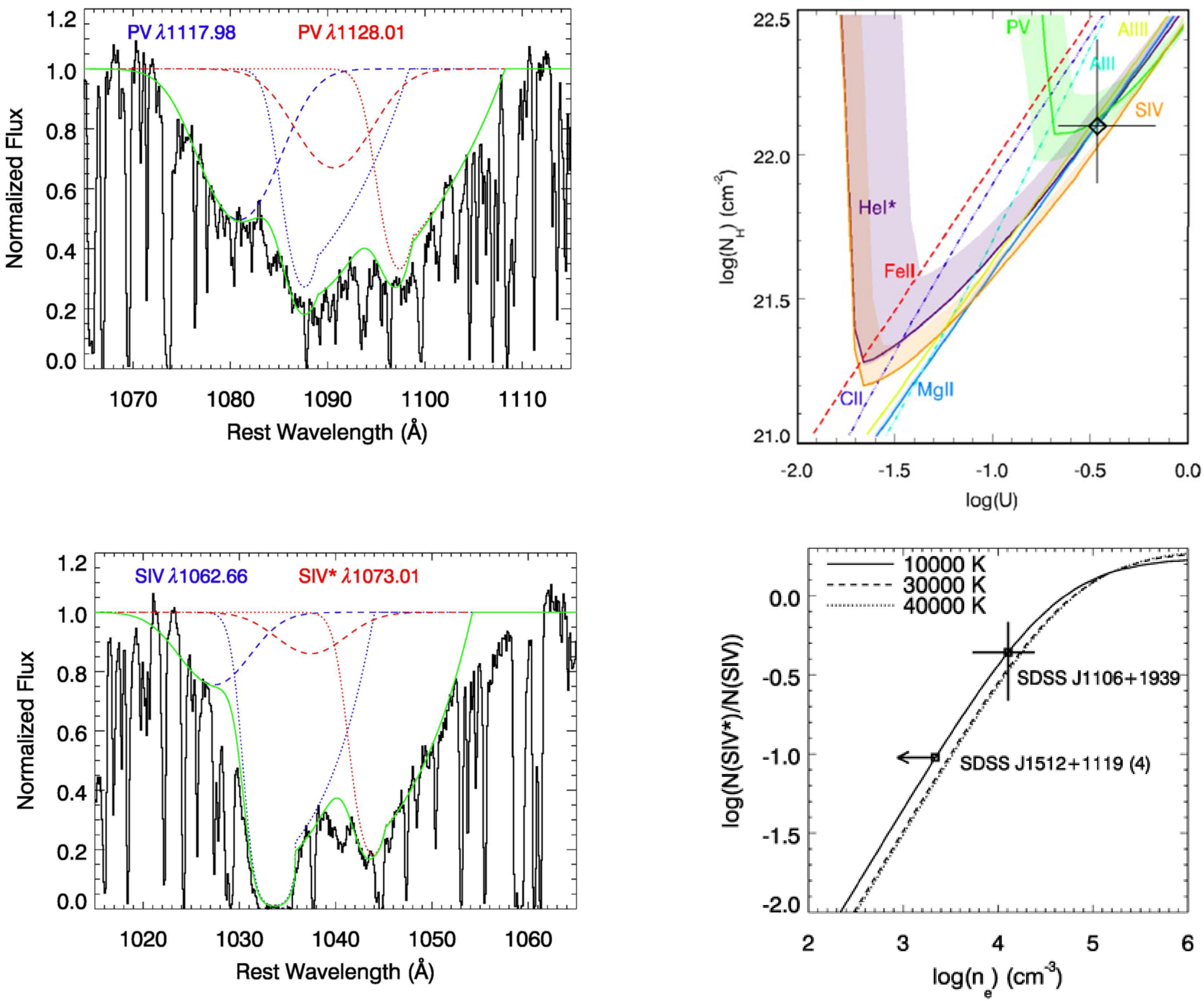
PV λ1117.98
PV λ1128.01
Normalized Flux
Rest Wavelength (Å)
PV
AlIII
AlII
SIV
HeI*
FeII
CII
MgII
log(N_H) (cm^-2)
log(U)
SIV λ1062.66
SIV* λ1073.01
Normalized Flux
Rest Wavelength (Å)
10000 K
30000 K
40000 K
SDSS J1106+1939
SDSS J1512+1119 (4)
log(N(SIV*)/N(SIV))
log(n_e) (cm^-3)

Object	$\log(L_{Bol})$ (ergs s^{-1})	v (km s^{-1})	$\log(U_H)$	$\log(N_H)$ (cm^{-2})	$\log(n_e)$ (cm^{-3})	R (kpc)	$\dot{M}$ (M$_\odot$ yr^{-1})	$\log(\dot{E}_k)$ (ergs s^{-1})	$\dot{E}_k / L_{EDD}$ (%)
J1106+1139 $4Z_\odot$	**47.2**	**-8250**	$-0.5^{+0.3}_{-0.2}$	$22.1^{+0.3}_{-0.1}$	$4.1^{+0.14}_{-0.37}$	$0.32^{+0.20}_{-0.14}$	390^{+300}_{-70}	$46.0^{+0.3}_{-0.1}$	5^{+4}_{-1}

Type equation here.

(Borguet + 2013)

Consequences for AGN feedback

- Over 10^7 years quasar duty cycle, such kinetic luminosity (10^{46} ergs/s) will yield a total kinetic energy of 10^{61} ergs. Enough to inflate the largest observed X-ray bubbles.

- Due to their larger opening angle and higher mass fluxes, absorption outflows may be more efficient for AGN feedback processes than AGN jets.

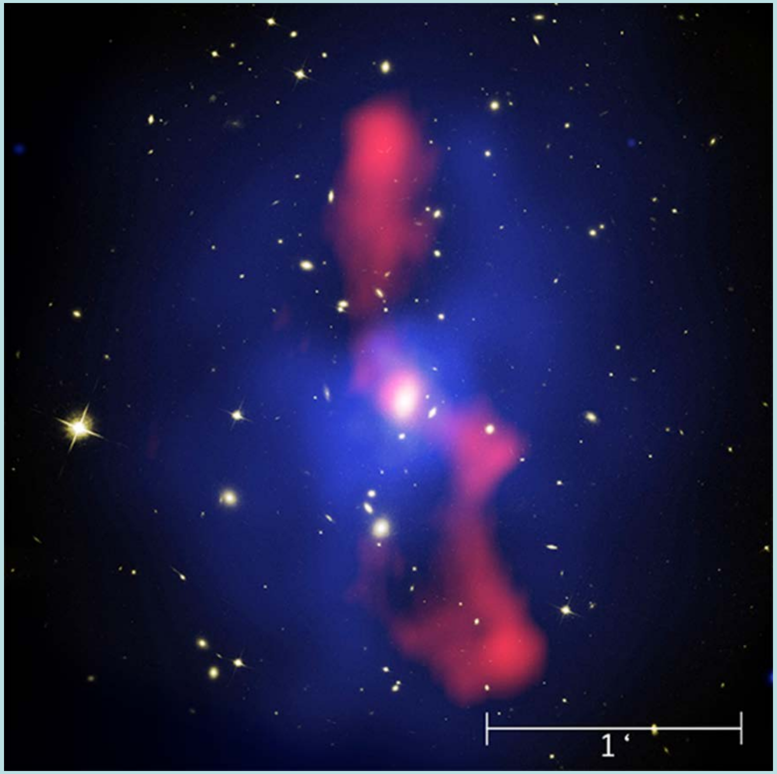

Absorption Summary

Kpc scale quasar outflows are a major component of AGN feedback, reaching kinetic luminosities of a few percent of L_{EDD}, with mass flux of hundreds of solar masses per year.

Object	v (km s^{-1})	R (pc)	$\dot{M}$ (M$_\odot$ yr^{-1})	Log $\dot{E}_k$ (erg s^{-1})	$\dot{E}_k/L^d_{\rm Edd}$ (per cent)	Ref
J0831+0354[1]	−10800	110[a]	135	45.7	5.2	1
J1106+1939[2]	−8250	320[a]	390	46.0	12	2
HE 0238−1904[3]	−5000	3400[b]	140	45.0	0.7	3
J0838+2955[4]	−5000	3300[c]	300	45.4	2.3	4
J0318−0600[5]	−4200	6000[c]	120	44.8	0.13	5

1) Chamberlain et al 2015 MNRAS in press (the above table, is table 1 in that paper)
2) Borguet et al., 2013, ApJ, 762, 49
3) Arav et al. 2013, MNRAS, 436, 3286A
4) Moe et al, 2009, ApJ, 706, 525
5) Dunn et al 2010, ApJ, 709, 611

Main weakness: Line of sight probe, spatial characteristics are statistically inferred

IFU observations

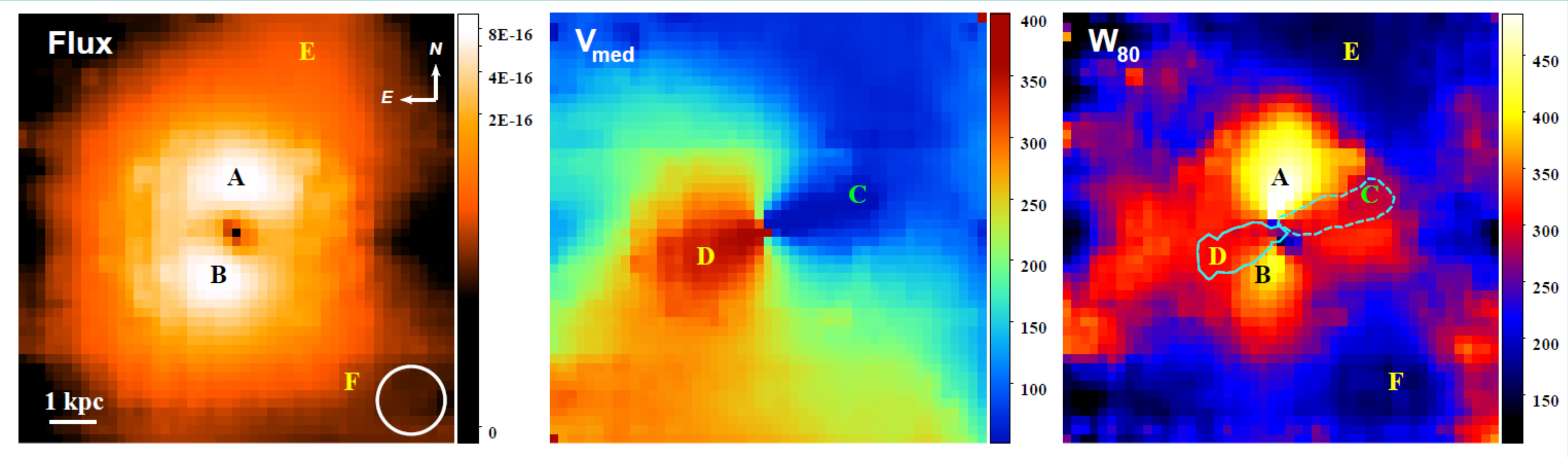

IRAS F04250−5718 *z*=0.1
(from Guilin + 2015)

“ the spatial locations, kinematics and energetics revealed by this IFU emission-line study are consistent with pre-existing UV absorption line analyses, providing a long-awaited direct confirmation of the atter as an effective approach for characterizing outflow properties.”

Spatial resolution and S/N

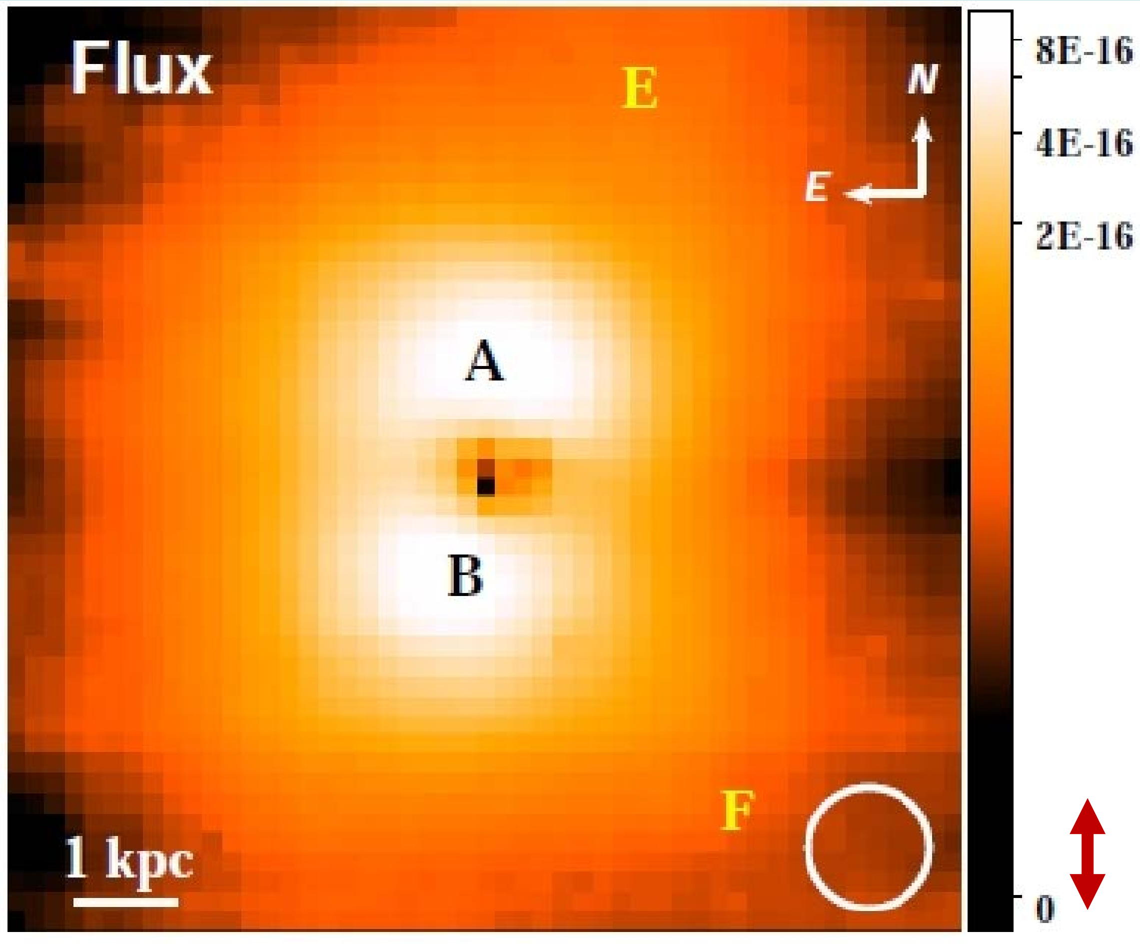

Serface brightness
Decreases as $(1+z)^{-4}$
Need large aperture

For 0.7<z<4
0.7 arcsec ~ 6 kpc

We need better than
1 kpc resolution

TMT IRIS

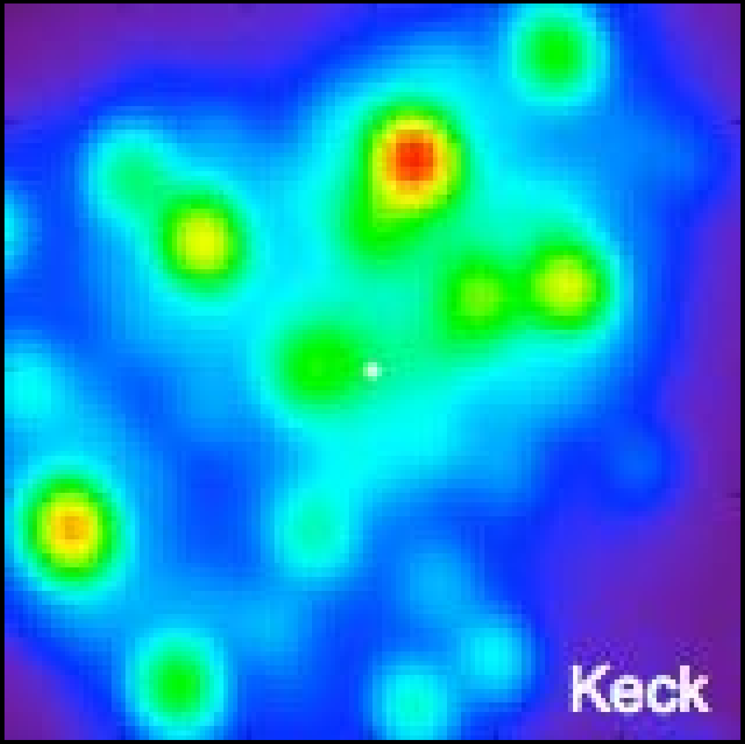

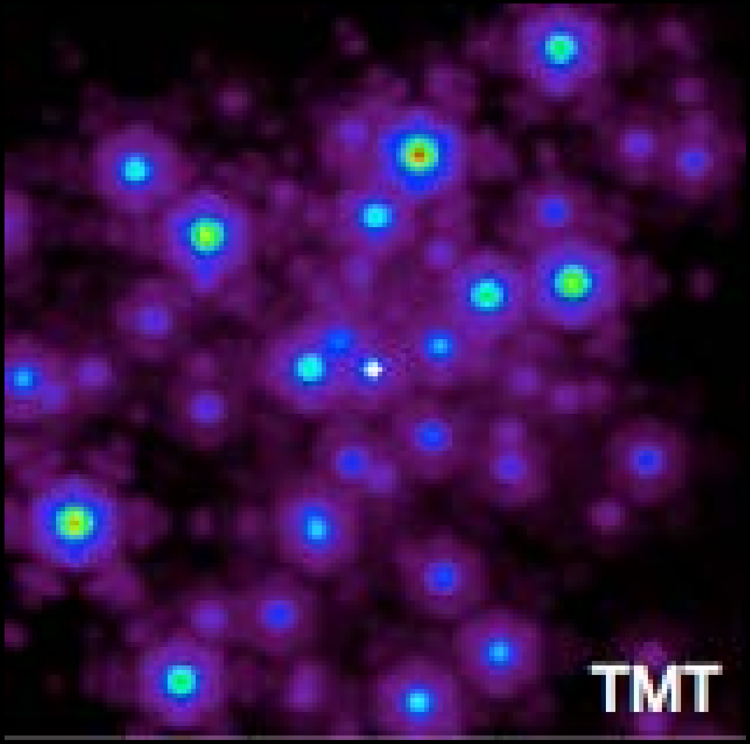

Simulations

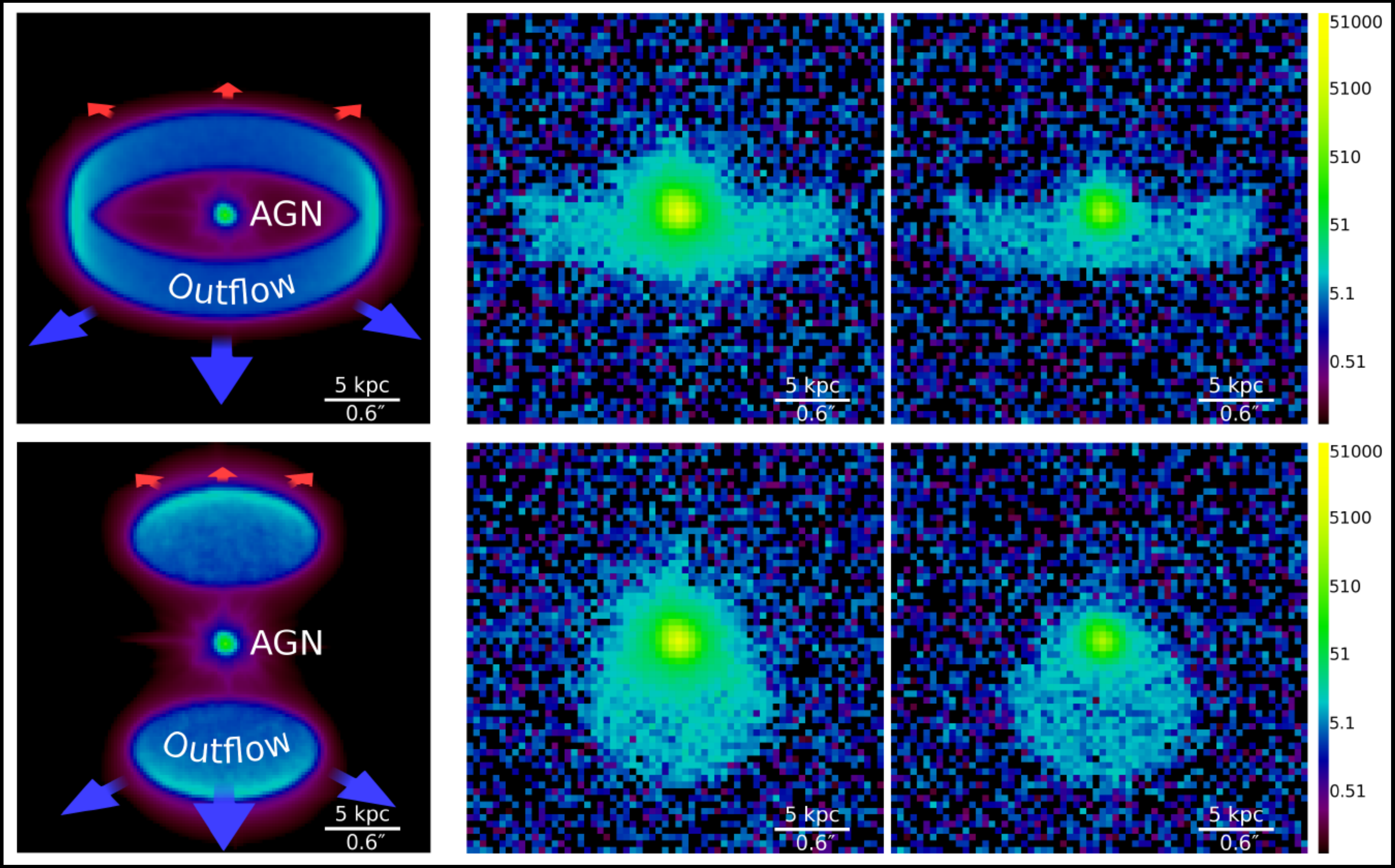

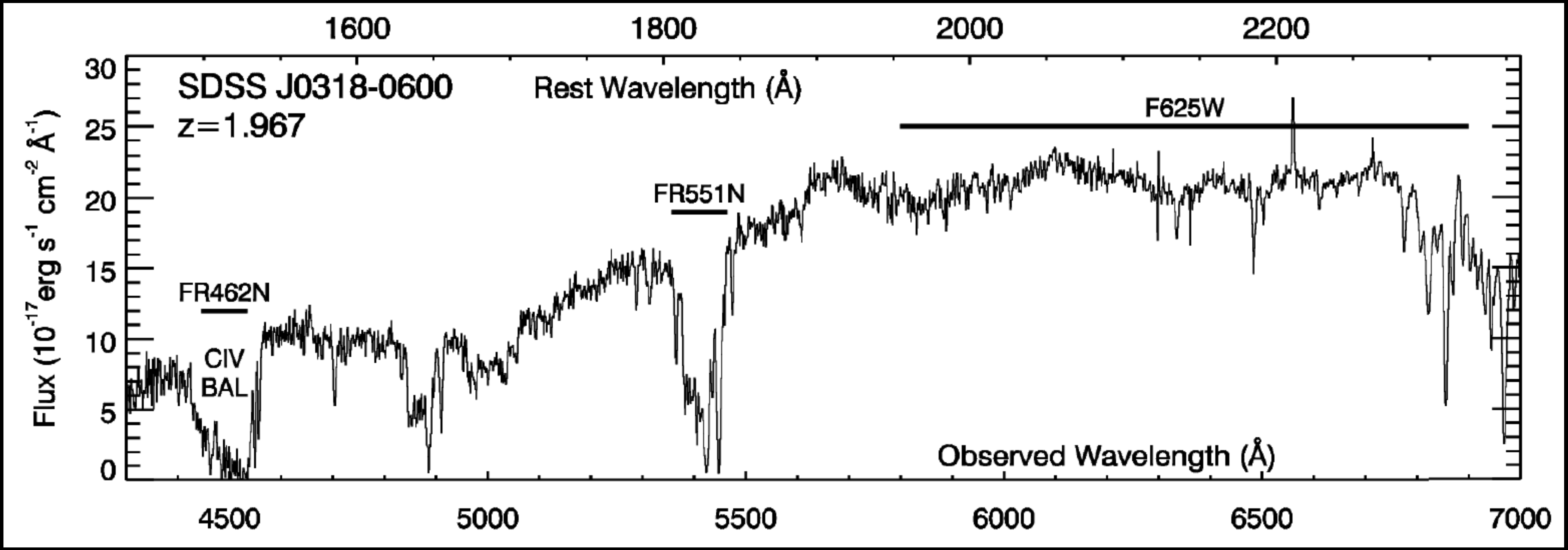

1600
1800
2000
2200
SDSS J0318-0600
z=1.967
Rest Wavelength (Å)
F625W
FR551N
FR462N
CIV
BAL
Flux (10^{-17} erg s^{-1} cm^{-2} Å^{-1})
30
25
20
15
10
5
0
Observed Wavelength (Å)
4500
5000
5500
6000
6500
7000

Quasars probing quasars outflows

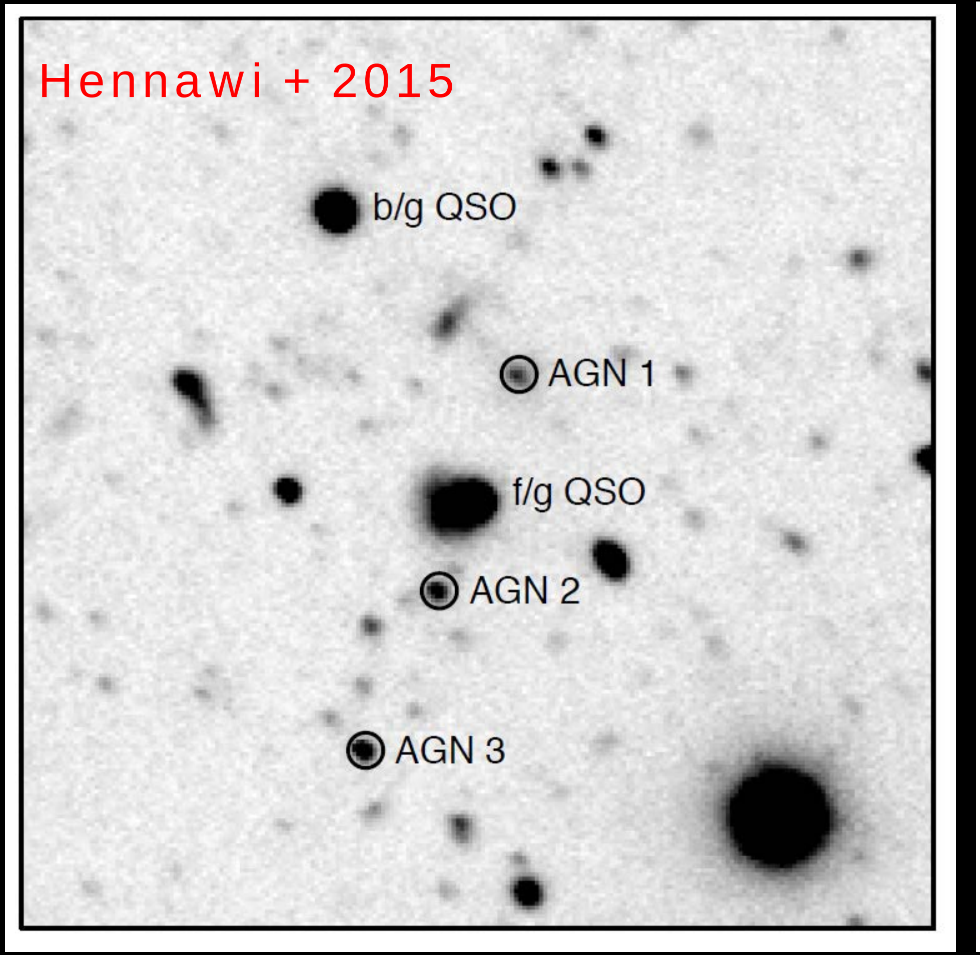

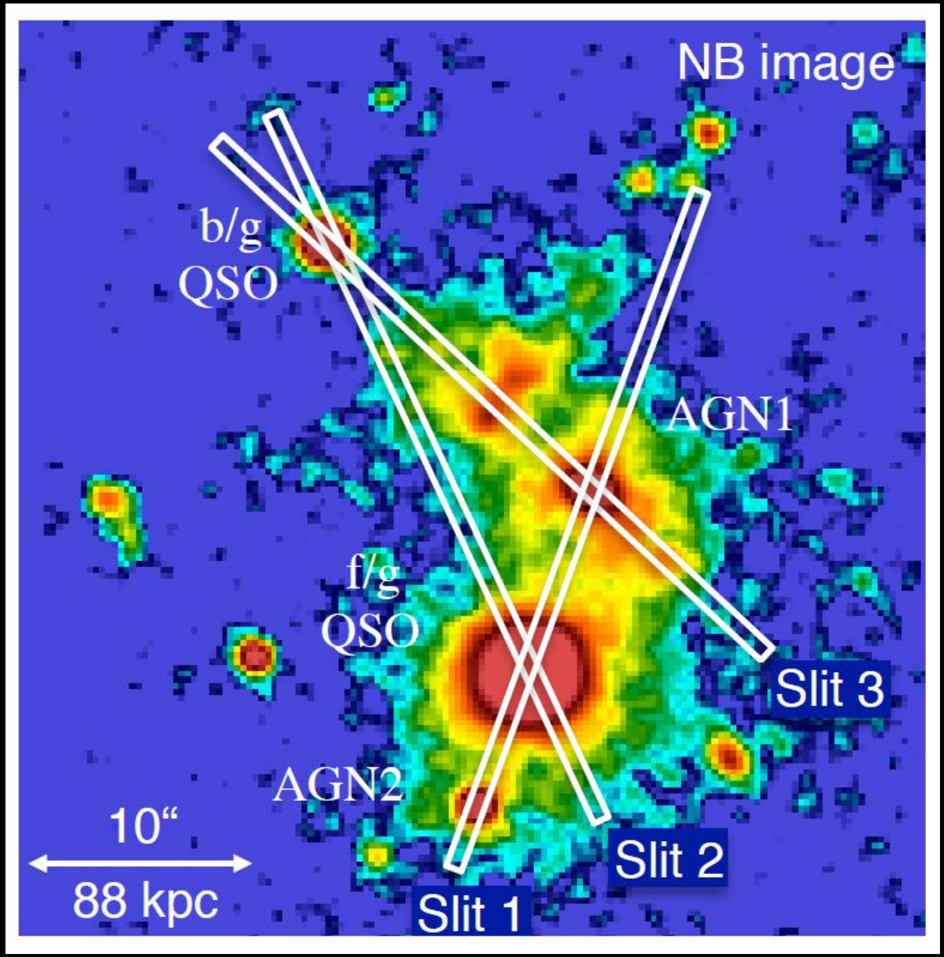

Great potential for InfraRed Multi-Object Spectrometer (IRMOS)

Summary

- TMT would immensely advance the connection between BALQSO and AGN feedback through:
- 1) High resolution high S/N IFU observations
- 2) Ability to obtain spectra from quasars with separated by less than 3 arcseconds